



## Search for $Wb\bar{b}$ and $WH$ Production in $p\bar{p}$ Collisions at $\sqrt{s} = 1.96$ TeV

The DØ Collaboration  
URL <http://www-d0.fnal.gov>  
(Dated: October 20, 2005)

We present results of a search for  $Wb\bar{b}$  production and for the Higgs boson through its  $b\bar{b}$  decay in the  $Wb\bar{b}$  channel in  $p\bar{p}$  collisions at  $\sqrt{s} = 1.96$  TeV at the Fermilab Tevatron. The search is conducted using events that contain one electron, missing transverse energy ( $\cancel{E}_T$ ), and two  $b$ -tagged jets observed in data corresponding to an integrated luminosity of  $382 \text{ pb}^{-1}$  accumulated in the DØ detector. A good description of candidate events as background originating from standard model processes provides a 95% C.L. upper limit on the  $Wb\bar{b}$  production cross section of 4.6 pb for  $b$ -quark transverse momenta  $p_T^b > 20$  GeV, pseudorapidity  $|\eta_b| < 2.5$ , and separation of the  $b\bar{b}$  system in  $(\eta, \phi)$  space  $\Delta R_{b\bar{b}} : \sqrt{\Delta\eta_{b\bar{b}}^2 + \Delta\phi_{b\bar{b}}^2} > 0.75$  where  $\Delta\eta_{b\bar{b}}$  and  $\Delta\phi_{b\bar{b}}$  correspond to the differences in pseudorapidities and azimuths of the  $b$  and  $\bar{b}$  candidates. In addition, since no excess of events is observed in the  $b\bar{b}$  invariant mass, we set 95% C.L. upper limits on the  $WH$  production cross section between 6.9 pb and 8.6 pb for Higgs boson masses between 105 and 135 GeV.

## I. INTRODUCTION

The Higgs mechanism is thought to be the agent of electroweak symmetry breaking in the standard model that is responsible for the observed masses of vector bosons and the elementary constituents. For this reason, finding the Higgs boson has been of primary importance in high energy physics experiments for the past decades. One of the cleanest search channels at the Tevatron  $p\bar{p}$  collider for Higgs boson masses of  $M_H < 140$  GeV is its production in association with a vector boson, where the vector boson undergoes a leptonic (electron) decay and the Higgs boson decays to a  $b\bar{b}$  pair. Since the expected production cross section for a Higgs boson associated with a  $W$ , when combined with leptonic branching ratio of the  $W$ , is significantly larger than that for associated production with a  $Z$  boson, the search for the Higgs boson in the final state of  $e\nu b\bar{b}$  is more promising. Results of previous searches in this final state for the Higgs boson and the production cross section measurement of its primary irreducible background process,  $Wb\bar{b}$ , using  $174 \text{ pb}^{-1}$  of data, have been published by the DØ collaboration [1] previously. This work updates the published result, and corresponds to a total integrated luminosity of  $382 \text{ pb}^{-1}$ . The current sample includes the entire previous data set, and has improved data quality.

## II. DATA SAMPLE

In this analysis, we make use of information from the DØ central-tracking system, which consists of a silicon microstrip tracker (SMT) and a central fiber tracker (CFT) situated inside a 2 T superconducting solenoidal magnet[2]. In addition, the analysis uses data from the liquid-argon/uranium calorimeter, which consists of a central calorimeter (CC) that covers  $|\eta| < 1.1$  ( $\eta = -\ln \tan \frac{\theta}{2}$ ) and two end calorimeters (EC), which extend the coverage to  $|\eta| < 4.2$ , housed in three independent cryostats. The transition regions ( $1.1 < |\eta| < 1.4$ ) of CC and EC are instrumented with scintillation counters that provide shower sampling of jet energies. Finally, for  $b$  tagging, the analysis exploits the muon system that surrounds the calorimeter and consists of a layer of drift tubes and scintillation trigger counters in front of a 1.8 T toroid, followed by two additional tracking layers outside the toroid for excellent muon momentum measurement.

Instantaneous luminosity is measured using scintillation counter arrays that are mounted in front of the EC cryostats, covering  $2.7 < |\eta| < 4.4$ . The trigger and data acquisition systems are designed to accommodate the high interaction rates of Run II.

Candidate events are required to pass one of the triggers that demand at least one electromagnetic (EM) object. The data are rejected if they are taken during periods in which the performance of any of the above systems is compromised. About 10% of all data is rejected due to this quality requirement. The resulting total integrated luminosity is  $382 \text{ pb}^{-1}$ . The uncertainty on the measured luminosity is 6.5%[3].

## III. EVENT SELECTION

As discussed in the introduction, the final state of the candidate events for this analysis contains one electron,  $\cancel{E}_T$  and two  $b$  jets. To select cleanest candidates, additional criteria are imposed. The candidate events are required to have a primary vertex  $z$  position within  $\pm 60$  cm of the nominal interaction point. In addition, events are required to contain an electron with  $p_T > 20$  GeV in the central region ( $|\eta| < 1.1$ ). The electrons must satisfy fiducial criteria to ensure full shower containment, and avoidance of cracks between azimuthal boundaries of electromagnetic(EM) calorimeter modules[4]. The electrons that pass the above kinematic and fiducial selections above are further required to satisfy more stringent identification criteria as follows:

- fractional energy in EM calorimeter over the total,  $f_{EM} = \frac{E_{EM}(0.2)}{E_{tot}(0.4)} > 0.9$ , where  $E_{tot}(0.4)$  and  $E_{EM}(0.2)$  are, respectively, the energies inside cone size 0.4 and 0.2, for the sum of hadronic and EM sections, and for EM section alone.
- isolation fraction,  $f_{iso} = \frac{E_{tot}(0.4) - E_{EM}(0.2)}{E_{EM}(0.2)} < 0.10$ ,
- seven-parameter electron shower shape variable,  $\chi_{HM7}^2 < 75$ ,
- electron likelihood  $[12] > 0.75$ .

In order to minimize backgrounds that contain two isolated leptons in the final state, such as from  $Z$  and  $t\bar{t}$  production, the candidate event is required to contain no isolated muons, or other electrons that satisfy the above criteria for  $p_T^e > 15$  GeV.

Events with candidate electrons that satisfy the electron identification criteria are then required to have  $\cancel{E}_T > 25$  GeV to enhance candidates with a  $W$  boson. The  $\cancel{E}_T$  used in this analysis is corrected for the presence of muons and for electron and jet energy scales. The candidate events are also required to contain just two jets reconstructed with a cone algorithm of radius  $\Delta R(= \sqrt{\Delta\eta^2 + \Delta\phi^2})=0.5$ . The jets are required to satisfy  $|\eta| < 2.5$  and  $p_T > 20$  GeV, after particle level energy scale corrections. A total of 3844 events satisfy the selection criteria up to this stage (Table I).

In order to distinguish  $Wb\bar{b}$  and  $WH$  candidates from ordinary  $W+2$  jet events whose jets originate from light quarks, we use the JLIP algorithm [5] to tag  $b$  jets. JLIP algorithm utilizes a “jet lifetime probability”, which is constructed from the tracks associated with jets that have positive impact parameters in the transverse plane, with the sign of the impact parameter defined by the scalar product  $\vec{d}_{perigee} \cdot \vec{p}_{T(jet)}$ , where  $\vec{d}_{perigee}$  is the distance vector in the transverse plane between the primary vertex and the point that defines the impact parameter. The jet lifetime probability is required to be consistent with that for a  $b$  jet. Only 153 events survive the requirement of having at least one  $b$ -tagged jet (Table I).

To enrich the  $Wb\bar{b}$  and  $WH$  content of the sample, the candidate events are now required to contain just two  $b$ -tagged jets. This reduces the sample to 13 events.

For consistency, all the above selection criteria are applied to data as well as to simulated events(see below).

#### IV. BACKGROUND ESTIMATES

The primary irreducible background sources for  $Wb\bar{b}$  and  $WH$  channels are from  $t\bar{t} \rightarrow ll\nu\nu b\bar{b}$ , in which  $l$  can be either an electron( $e$ ) or muon( $\mu$ ), including indirect  $e$  or  $\mu$  from  $\tau$  decays, single top production( $t\bar{b} \rightarrow e\nu b\bar{b}$ ), and  $WZ \rightarrow e\nu b\bar{b}$ .  $Wb\bar{b}$  is one of the primary irreducible backgrounds to the  $WH$  channel. Other background sources that contain signatures considered in this analysis include  $W(\rightarrow e\nu)+2$  jets, where both jets are misidentified as  $b$  jets. We also consider three additional channels with two light jets misidentified as  $b$  jets,  $W(\rightarrow \tau\nu \rightarrow e\nu\nu)+2$  jets,  $Z(\rightarrow \tau\tau \rightarrow e\nu\nu + \text{hadrons})+2$  jets, and  $Z(\rightarrow ee)+2$  jets, in which one of the electrons is lost, and the  $\cancel{E}_T$  is introduced from an incomplete measurement of the total transverse energy.

Fully simulated Monte Carlo (MC) samples are used to estimate background contributions from the irreducible processes. Of the MC samples, the following processes are generated with PYTHIA[6] v6.202, using CTEQ5L[7] leading-order (LO) parton distribution functions (PDF):

- inclusive production of  $Z \rightarrow ee$ ,  $W \rightarrow \tau\nu$ ,  $Z \rightarrow \tau\tau$ , and  $WZ(W \rightarrow e\nu, Z \rightarrow b\bar{b})$
- $t\bar{t} \rightarrow l\nu + 2 \text{ jets} + b\bar{b}$  and  $t\bar{t} \rightarrow ll\nu\nu + b\bar{b}$
- $WH \rightarrow e\nu + b\bar{b}$

Because PYTHIA does not provide an adequate description of heavy-quark productions and higher-order processes with larger jet multiplicities, the following processes are generated using other generators:

- single-top (s-channel and t-channel) events are generated using COMPHEP[8]
- $W + \text{jets}$  (excluding  $b$  jets) and  $W + b\bar{b}$  events are generated with ALPGEN, requiring 2 parton jets with  $p_T > 8$  GeV, separated by  $\Delta R > 0.4$

These events are then passed through the PYTHIA parton-showering and hadronization process, followed by full detector simulation. We use the next-to-leading order cross section wherever available. We assign 18% systematic uncertainty on the cross sections due to uncertainties in PDF and dependence on renormalization and factorization scales in leading-order calculations[9].

Instrumental background from multijet events in which one of the jets is misidentified as an electron and two other jets are either mistaken as  $b$  jets or are  $b\bar{b}$  pair produced from gluon splitting, are estimated from data using measured probabilities of electron reconstruction and misidentification of jets as electrons. The probability that a jet mimics an electron was estimated from data that contain 2 back-to-back jets with low  $\cancel{E}_T$  to minimize contamination from true  $W$  bosons in the sample. One of the two jets is required to have an EM fraction  $f_{EM} < 0.7$  to select a hadronic jet and to be in the CC away from EM module boundaries, to avoid artificial  $\cancel{E}_T$  from mismeasurement of transverse momentum. The remaining jet is required to satisfy all electron requirements, except the electron likelihood selection which, as a result, defines a false candidate electron. Using this method the probability of a false candidate passing the electron likelihood requirement is measured to be  $(11 \pm 3)\%$  [9].

Except for the  $Wjj$  background, the expected numbers of events for simulated reactions are calculated from Monte Carlo samples and represent absolute predictions. The estimated number of  $Wjj$  events is obtained by subtracting the expected numbers of all other background sources that have an electron,  $\cancel{E}_T$  and 2 jets in the event (such as in

$t\bar{t}$  and single-top production) from the number observed in data, before requiring  $b$  tagging. At this stage, the sum of all other backgrounds is small compared to  $Wjj$ , except for multijets. The normalization factor obtained at this stage is used in the later analysis when  $b$  tagging is implemented.

Table I summarizes the estimated contributions from all processes to samples at different stages of analysis. The combined uncertainties associated with the background contributions in the table reflect both the MC statistics and systematic uncertainties, including 18% uncertainty in MC cross sections. In Figs. 1a and 1b we show the  $p_T$  and  $\eta$  distributions of electrons in the  $W+2$  jet candidate events. The  $\cancel{E}_T$  and the  $(e, \cancel{E}_T)$  transverse mass distributions of candidate events are shown in Figs. 1c and 1d, demonstrating good agreement of expectation with data. In Figs. 2a and 2b we show the  $p_T$  distributions of the leading and next-to-leading jet in the selected sample, respectively. In Figs. 2c and 2d we show the  $p_T$  distributions of the  $b$ -tagged jets and the invariant mass of the di-jet in events with at least one  $b$ -tagged jet. Analogous distributions for events with both jets tagged as  $b$  jets are shown in Figs. 3a and 3b.

The electron ID/reconstruction efficiency is estimated using  $Z \rightarrow ee$  candidate events in data. The efficiency for electron likelihood selection for  $|\eta| < 1.1$  is found to be  $(91 \pm 3)\%$  [9]. The mean efficiency for the entire CC is found to be  $(74 \pm 4)\%$ . Jet ID/reconstruction efficiency is estimated using QCD multijet MC event samples. The jet ID/reconstruction efficiency is  $(95 \pm 5)\%$  for  $p_T > 20$  GeV. The ratio of efficiencies for data to MC is parameterized as a function of jet  $p_T$  and is used to re-weight the simulated events. For the jet  $b$ -lifetime probability used in this analysis, the mistag rate (tagging of light quarks) is  $(0.5 \pm 0.05)\%$  [10], and the  $b$ -tagging efficiency for a “taggable” jet is found to be  $48 \pm 3\%$  [9]. (A jet is “taggable” if at least one track can be associated with it. Approximately 80% of jets in multijet events are taggable.[10].) The ratio between data and MC for the taggability  $\times$  tagging efficiency  $(0.88 \times 0.78)$  is used to reweight every  $b$ -tagged jet in simulated events.

## V. RESULT OF $Wb\bar{b}$ SEARCH

A 1%  $Wb\bar{b}$  signal acceptance is obtained using a full detector simulation of MC events generated with ALPGEN. The overall systematic uncertainty on the signal acceptance is 16.2%. The contributions from different sources given in Table II. Most of the systematic uncertainties are retained from the previous study [9], except for those due to jet energy scale (JES) and trigger efficiencies. Because the overall systematic uncertainty from MC is assumed to be the same for both signal and background, we assign a combined uncertainty of 24.0% to the estimation of background and signal, which corresponds to a sum in quadrature of an 18% uncertainty on the cross section and the uncertainty on acceptance. In addition, we assign a 40% systematic uncertainty to multijet background in the double- $b$ -tagged sample. The two primary sources that contribute to this uncertainty are: 22% from the uncertainty of false-electron probability and 33% from the statistical uncertainty in the control sample used to obtain the probability.

A total of 13 events are left in the sample after all selection criteria are applied. Figures 3a and 3c show the  $b$  jet  $p_T$  and the  $(e, \cancel{E}_T)$  transverse mass distributions, respectively, while 3b and 3d show the  $b\bar{b}$  invariant mass distributions of these 13 events using linear and semi-log scale, along with expected contributions. The total background to  $Wb\bar{b}$  is estimated to be  $5.73 \pm 1.45$ . The upper limit on the  $Wb\bar{b}$  production cross section is obtained using a Bayesian limit calculation method. The 95 % C.L. upper limit on  $Wb\bar{b}$  production obtained from this analysis is 4.6 pb for  $b$  jets with  $p_T^b > 20$  GeV,  $|\eta^b| < 2.5$  and  $\Delta R_{b\bar{b}} > 0.75$ .

## VI. SEARCH FOR $WH$ PRODUCTION

In order to minimize  $Wb\bar{b}$  background contributions to a potential Higgs signal, we apply an additional selection on the  $b\bar{b}$  invariant mass, using a window that slides along with the mass of the Higgs boson. For  $M_H=115$  GeV, a total of 4 events are observed in the mass window  $85 < M_{b\bar{b}} < 135$  GeV, with  $2.37 \pm 0.59$  expected from background.

Since no excess is observed at  $M_H=115$  GeV, we set an upper limit on the  $WH$  production cross section. The signal acceptance for  $WH$  is  $(0.23 \pm 0.03)\%$ . The 95 % C.L. upper limit on the  $WH$  ( $M_H=115$  GeV) production cross section is found to be 8.6 pb.

We also investigated other Higgs mass points;  $M_H=105, 125$  and  $135$  GeV. For all these mass points, we observe no excess over the estimated background. The 95% C.L. upper limits for cross sections vary from 6.9 pb to 7.6 pb for these masses. The mass window, the resulting number of candidate events in data, the background estimate, and the 95% C.L. upper limits on cross section are summarized in Table III. Figure 4 shows the cross section upper limits from this analysis as a function of Higgs mass.

Although we do not observe any excess in the Higgs signal region, we observe a small excess in the high  $b\bar{b}$  invariant mass region. For instance for  $m_{b\bar{b}} > 150$  GeV a total of seven events are observed with  $2.1 \pm 0.5$  expected. Different

	$W + 2 \text{ jets}$	$W + \geq 1 \text{ } b$	$W + 2 \text{ } b$	$W + 2 \text{ } b$ $85 < m_{b\bar{b}} < 135 \text{ GeV}$
$Wb\bar{b}$	$44.8 \pm 10.7$	$18.1 \pm 4.3$	$4.29 \pm 1.03$	$1.10 \pm 0.26$
$WH$	$0.94 \pm 0.2$	$0.44 \pm 0.1$	$0.14 \pm 0.03$	$0.12 \pm 0.03$
$WZ$	$2.6 \pm 0.6$	$1.1 \pm 0.3$	$0.33 \pm 0.08$	$0.17 \pm 0.04$
$t\bar{t}$	$22.0 \pm 5.3$	$9.5 \pm 2.3$	$2.23 \pm 0.54$	$0.61 \pm 0.15$
Single top	$16.8 \pm 0.4$	$6.8 \pm 1.6$	$1.11 \pm 0.27$	$0.35 \pm 0.08$
Multijets	$474 \pm 104$	$23 \pm 5$	$0.42 \pm 0.17$	$0.14 \pm 0.06$
$W/Z$ +jets	$3256 \pm 781$	$95.1 \pm 23$	$1.64 \pm 0.39$	0.0
Total background	$3771 \pm 911$	$135.5 \pm 33$	$5.73 \pm 1.45$	$2.37 \pm 0.59$
Total expectation	$3816 \pm 921$	$153.6 \pm 38$	$10.2 \pm 2.4$	$2.49 \pm 0.62$
Data	3844	153	13	4

TABLE I: Summary of expected  $Wb\bar{b}$  and  $WH$  and background events at various stages of the analysis for different requirements on jets. The  $t\bar{t}$  background contains both single-lepton+jets and dilepton samples, and  $W/Z$ +jets represents background from  $Wjj$  and  $W$  and  $Z$  inclusive samples. The  $b\bar{b}$  invariant mass window in the last column is 85 - 135 GeV for  $M_H = 115$  GeV. The total expectation is sum of the total background and signal( $Wb\bar{b}$  and  $WH$ ).

Sources	Uncertainty
Trigger efficiency	3%
Electron likelihood efficiency	3%
Electron ID/Reconstruction Efficiency	3%
Electron energy uncertainty (energy smearing)	4 (1)%
Jet ID/Reconstruction Efficiency	5%
Jet Multiplicity	3%
MLM Matching	4%
Jet Energy Scale (JES)	4 (7 for WH)%
Jet Taggability	4%
JLIP Efficiency	10%

TABLE II: Summary of systematic uncertainties for signal acceptance. By MLM Matching[11], we mean an inclusive prescription for removing PYTHIA parton showers with higher  $p_T$  than expected in ALPGEN.

sources for this excess have been investigated (multijet production or other processes such as  $t\bar{t}$  and single top), and we conclude that this excess is likely to be a statistical fluctuation from the combined background sources.

## VII. SUMMARY

We have searched for  $Wb\bar{b}$  and  $WH$  production in final states that contain one high  $p_T$  electron,  $\cancel{E}_T$  and two  $b$  jets, using data that corresponds to a total integrated luminosity of  $382 \text{ pb}^{-1}$ . Detailed comparisons of data and background estimated from the standard model show no excess above expectation. The  $Wb\bar{b}$  production cross section 95% C.L. upper limit is set at 4.6 pb for  $b$  jets with  $p_T^b > 20 \text{ GeV}$ ,  $|\eta^{b-jet}| < 2.5$  and  $\Delta R_{b\bar{b}} > 0.75$ . In addition, a search for the Higgs boson in the  $b\bar{b}$  invariant mass shows no excess of events above the background in the mass range of  $105 < M_H < 135 \text{ GeV}$ . From these results, we obtain 95% C.L. upper limits between 6.9 pb and 8.6 pb on  $\sigma(p\bar{p} \rightarrow WH) \times B(H \rightarrow b\bar{b})$  for  $M_H$  between 105 GeV and 135 GeV.

	105 GeV	115 GeV	125 GeV	135 GeV
$WH$	$0.14 \pm 0.03$	$0.12 \pm 0.03$	$0.07 \pm 0.02$	$0.04 \pm 0.01$
$Wb\bar{b}$	$1.40 \pm 0.34$	$1.10 \pm 0.26$	$0.96 \pm 0.23$	$0.72 \pm 0.17$
$WZ$	$0.25 \pm 0.49$	$0.17 \pm 0.04$	$0.07 \pm 0.02$	$0.02 \pm 0.005$
$t\bar{t}$	$0.58 \pm 0.14$	$0.61 \pm 0.15$	$0.64 \pm 0.15$	$0.63 \pm 0.15$
Single top	$0.34 \pm 0.08$	$0.35 \pm 0.08$	$0.32 \pm 0.08$	$0.31 \pm 0.08$
Multijets and $W/Z$ +jets	$0.59 \pm 0.17$	$0.14 \pm 0.06$	$0.14 \pm 0.06$	$0.12 \pm 0.05$
Total backgrounds	$3.16 \pm 1.22$	$2.37 \pm 0.59$	$2.13 \pm 0.5$	$1.8 \pm 0.5$
Efficiency(%)	$0.184 \pm 0.03$	$0.23 \pm 0.03$	$0.24 \pm 0.03$	$0.26 \pm 0.04$
Events observed	2	4	3	3
U.L. at 95 % C.L.	7.4 pb	8.6 pb	7.0 pb	6.9 pb
Expected U.L.	9.0 pb	5.7 pb	5.6 pb	4.3 pb

TABLE III: Summary of  $WH$  analysis. Expected number of  $WH$  events and background contributions for  $M_h=105, 115, 125$  and 135 GeV, along with 95% C.L. cross section upper limits. (U.L. stands for Upper Limit and C.L. stands for Confidence Level.)

### Acknowledgments

We thank the staffs at Fermilab and collaborating institutions, and acknowledge support from the DOE and NSF (USA), CEA and CNRS/IN2P3 (France), Ministry of Education and Science, Agency for Atomic Energy and RF President Grants Program (Russia), CAPES, CNPq, FAPERJ, FAPESP and FUNDUNESP (Brazil), Departments of Atomic Energy and Science and Technology (India), Colciencias (Colombia), CONACyT (Mexico), KRF (Korea), CONICET and UBACyT (Argentina), The Foundation for Fundamental Research on Matter (The Netherlands), PPARC (United Kingdom), Ministry of Education (Czech Republic), Canada Research Chairs Program, CFI, Natural Sciences and Engineering Research Council and WestGrid Project (Canada), BMBF and DFG (Germany), Science Foundation Ireland, A.P. Sloan Foundation, Research Corporation, Texas Advanced Research Program, Alexander von Humboldt Foundation, and the Marie Curie Fellowships.

- 
- [1] Phys. Rev. Letters 94, 091802(2005), A Search for  $Wb\bar{b}$  and  $WH$  production in  $p\bar{p}$  Collisions at  $\sqrt{s} = 1.96$  TeV DØ Collaboration, 2005.
  - [2] V. Abazov, et al., in preparation for submission to Nucl. Instrum. Methods Phys. res. A, and T. LeCompte and H.T. Diehl, “The CDF and D0 Upgrades for Run II”, Ann. Rev. Nucl. Part. Sci. 50, 71 (2000).
  - [3] Luminosity ID group : [http://www-d0.fnal.gov/phys\\_id/luminosity/data\\_excess/](http://www-d0.fnal.gov/phys_id/luminosity/data_excess/).
  - [4] EM-ID group, Certification Results Version 5.0, [http://www-d0.fnal.gov/phys\\_id/emid/d0\\_private/certification/](http://www-d0.fnal.gov/phys_id/emid/d0_private/certification/).
  - [5] D. Bloch et al., Jet Lifetime  $b$  Tagging , DØ Note 4069.
  - [6] T. Sjostrand, P. Eden, C. Friberg, G. Miu, S. Mrenna and E. Norrbin, “High-energy-physics event generation with PYTHIA,” Comput. Phys. Commun. 135, (2001) 238.
  - [7] H.L.Lai et al., Improved Parton Distribution from Global Analysis of Recent Deep Inelastic Scattering and Inclusive Jet Data, Phys. rev. D55(1997) 1280.
  - [8] A. Pukhov et al., COMPHEP, hep-ph/9908288(1999).
  - [9] D0 Note 4394, Search for  $Wb\bar{b}$  and  $WH$  Production in  $p\bar{p}$  Collisions at  $\sqrt{s} = 1.96$  TeV. S. Beauceron and G. Bernardi, 2004.
  - [10] [http://www-d0.fnal.gov/phys\\_id/bid/d0\\_private/certification/p14Pass2/JLIP/Jetprob\\_v1.html](http://www-d0.fnal.gov/phys_id/bid/d0_private/certification/p14Pass2/JLIP/Jetprob_v1.html).
  - [11] M. L. Mangano, “Exploring theoretical systematics in the ME-to-Shower MC merging for multijet process”, E-proceedings of Matrix Element/Monte Carlo Tuning Working Group, Fermilab, November 2002.
  - [12] 7 variables include spatial track match  $\chi^2$  probability,  $E_T/p_T$ , H-matrix7, EMF, distance of closest approach to primary vertex, number of tracks in 0.05 cone, total  $p_T$  of tracks in 0.4 cone around candidate track.

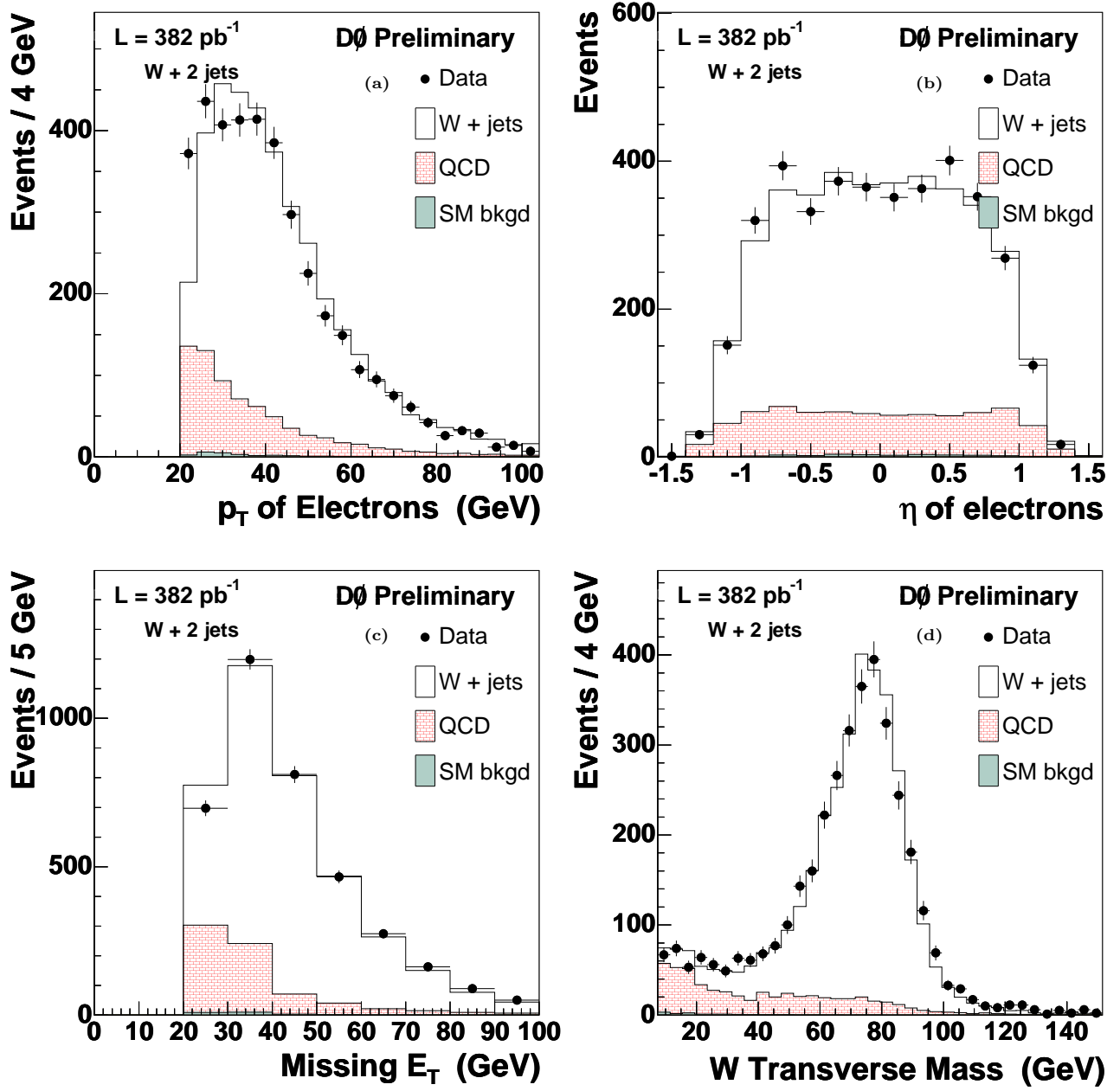


FIG. 1: Kinematic distributions for the  $W + jj$  sample: a) transverse momentum of electrons, b)  $\eta$  distribution of electrons, c) missing transverse energy; d) transverse mass of  $e$  and  $\cancel{E}_T$ . The background from MC simulation is normalized to the integrated luminosity of the data sample using the calculated cross sections (absolute normalization), except for the  $Wjj$  contribution, which is normalized such that the sum of all backgrounds equals the number of observed events (see the text). Background from multijet production is estimated from data.

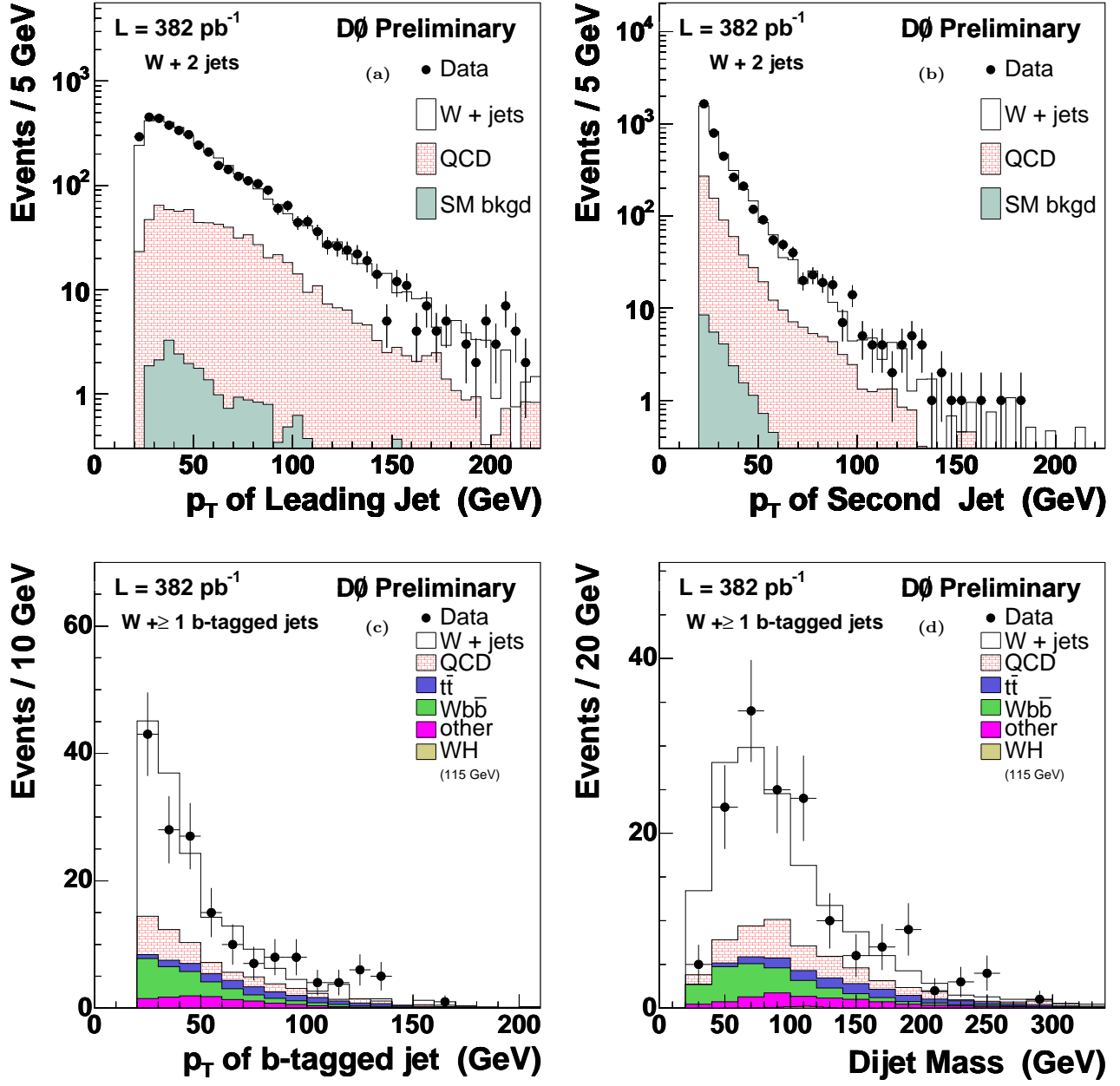


FIG. 2: Kinematic distributions for jets in the  $W + jj$  sample: a) leading jet  $p_T$ , b) next-to-leading jet  $p_T$ , and where at least one jet is  $b$ -tagged: c) transverse momentum of the  $b$ -tagged jet, d) the invariant mass of the two jets in the event. The normalization used in these plots is same as in Fig. 1.



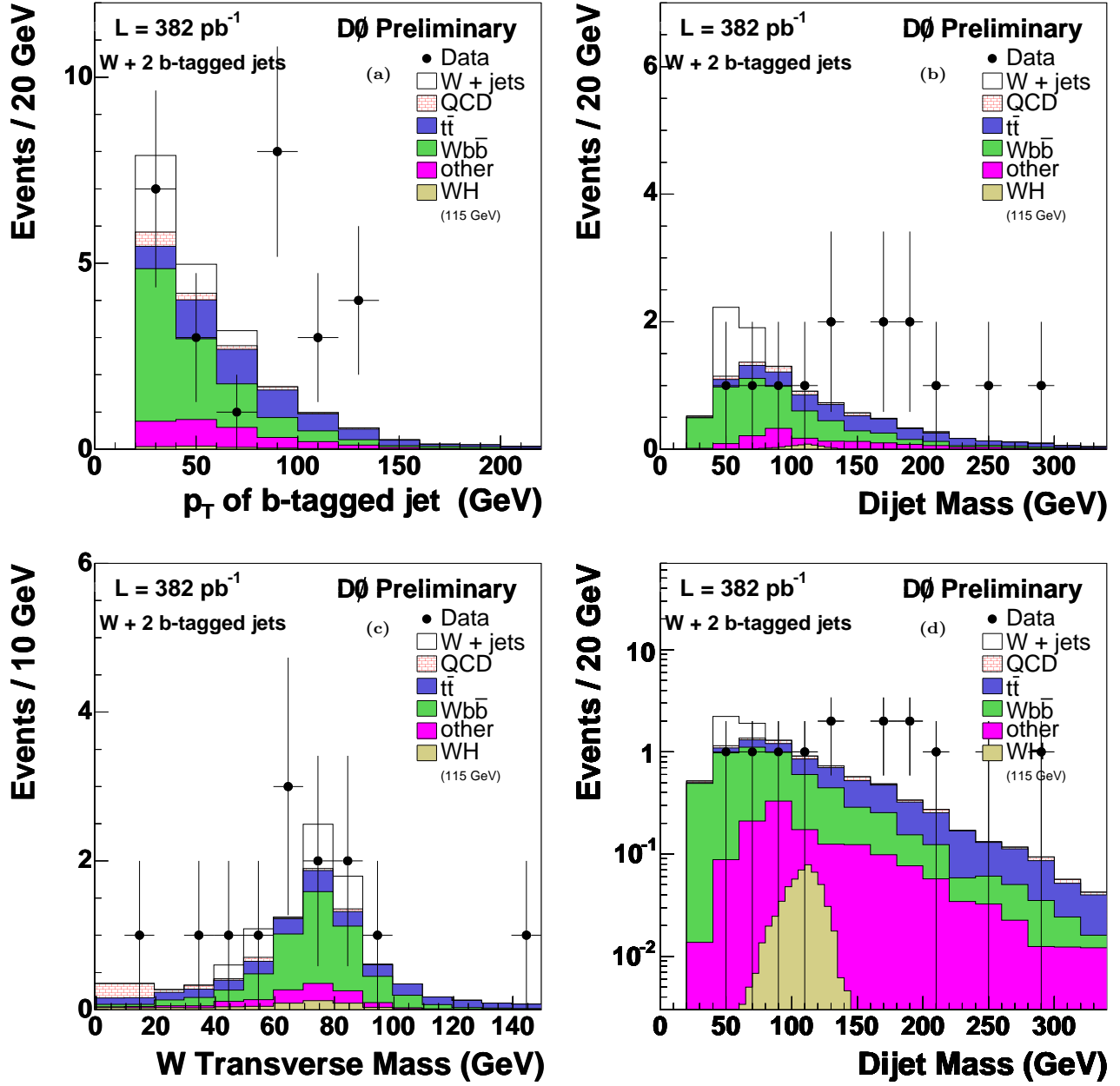


FIG. 3: Distributions for  $W + 2 b$  jets events: a) transverse momentum of  $b$ -tagged jets, b) di-jet invariant mass on a linear scale c) transverse mass of  $e$  and  $\cancel{E}_T$  system, d) di-jet invariant mass on a log scale. The contribution from a 115 GeV Higgs Boson is shown with finer binning (5 GeV) and multiplied by a factor of 4. The mean and RMS of this signal is 110 GeV and 16 GeV, respectively, resulting in a relative mass resolution of 14 % [1]. The normalization used in these plots is same as in Fig. 1.

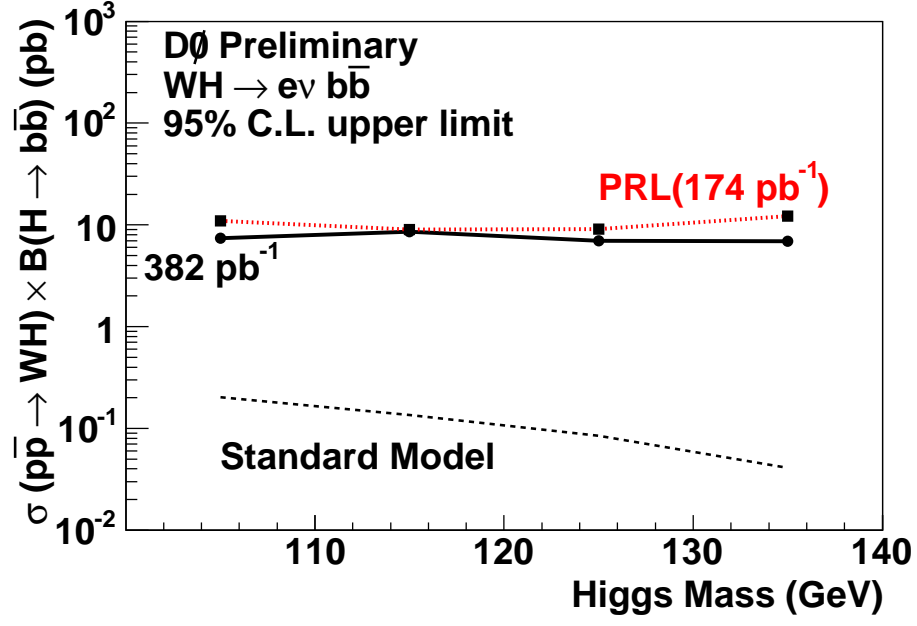


FIG. 4: 95 % C.L. upper limits on the product of the  $WH$  production cross section and the branching fraction of  $H \rightarrow b\bar{b}$  as a function of Higgs mass are shown for the results of this analysis(circles), and the previous published study[1](boxes). Also shown is the the prediction of the standard model as a function of Higgs mass.